



TITLE:

Particle Scattering Function for Spherical Block Copolymer Micelles (Commemoration Issue Dedicated to Professor Keinosuke Kobayashi on the Occasion of His Retirement)

AUTHOR(S):

Tanaka, Takeshi; Kotaka, Tadado; Inagaki, Hiroshi

CITATION:

Tanaka, Takeshi ...[et al]. Particle Scattering Function for Spherical Block Copolymer Micelles (Commemoration Issue Dedicated to Professor Keinosuke Kobayashi on the Occasion of His Retirement). Bulletin of the Institute for Chemical Research, Kyoto University 1977, 55(2): 206-216

ISSUE DATE:

1977-08-31

URL:

<http://hdl.handle.net/2433/76727>

RIGHT:

Particle Scattering Function for Spherical Block Copolymer Micelles

Takeshi TANAKA, Tadao KOTAKA†, and Hiroshi INAGAKI*

Received April 14, 1977

The Debye particle scattering function P was calculated on the "three-phase model" representing a spherical multimolecular micelle formed by an AB diblock copolymer. The model consists of the three phases, *i.e.*, a pure B phase forming the spherical "core", an A-B intermixing phase forming the "shell" in which the A-B junctions are located, and a pure A phase forming the "fringe" surrounding the shell and the core. The A chains were assumed to obey the statistics of the random-flight chain with one end (*i.e.*, the junction) bound near the impermeable surface (of the B core). The calculations showed that the P^{-1} vs $C \sin^2 (\theta/2)$ curve with the constant C so chosen as to give the initial slope of $1/3$ increases with increasing angle much more rapidly than that for the linear chain, but less rapidly than that for the uniform-density model, essentially in agreement with observations. The method to analyze, on the basis of the model, experimental data obtained from the core-component-invisible micelle systems was discussed. It was shown that new information about the micelle morphology is obtainable. Above all, the extent of expansion of the A chains in the radial direction could be determined with little (theoretical) ambiguity.

INTRODUCTION

The formation of multimolecular micelles by block and graft copolymers in the presence of a selectively bad solvent for one of the copolymer components is well known.¹⁾ Figure 1 will give an idea about such micelles. It shows electron micrographs of the micelles formed by polystyrene (PS)-poly(methyl methacrylate) (PM) diblock copolymers in acetonitrile solution.²⁾ Spherical micelles nearly uniform in size are seen. Each micelle is considered to consist of several hundreds of molecules. In general, a micelle formed by a diblock copolymer in a selective solvent may be considered to consist of a compact core (swollen to a certain extent) of the less soluble component surrounded by a flexible fringe of the more soluble component which maintains the system in a colloidal state. In the above example, acetonitrile is a nonsolvent for PS and a near- Θ solvent for PM at the room temperature, so that the micelle surface consists predominantly of the PM chains.²⁾

The electron micrographic morphology is, of course, different from that in solution, because polymer coils will collapse upon themselves during the solvent evaporation stage. Direct morphological information comes from the light scattering investigation of the particle scattering function P . Previously, we³⁾ proposed a model representing a spherical micelle formed by an AB diblock copolymer, and calculated the P function of the model. The "star-shape model", so called in the paper, has a seemingly unrealistic aspect: The A chains forming the fringe with one end fixed on the surface of the spherical core formed

* 田中 猛, 小高忠男, 稲垣 博: Laboratory of Polymer Separation and Characterization, Institute for Chemical Research, Kyoto University, Uji, Kyoto-Fu 611.

† Present Address: Department of Polymer Science, Osaka University, Toyonaka, Osaka-Fu 560, Japan.

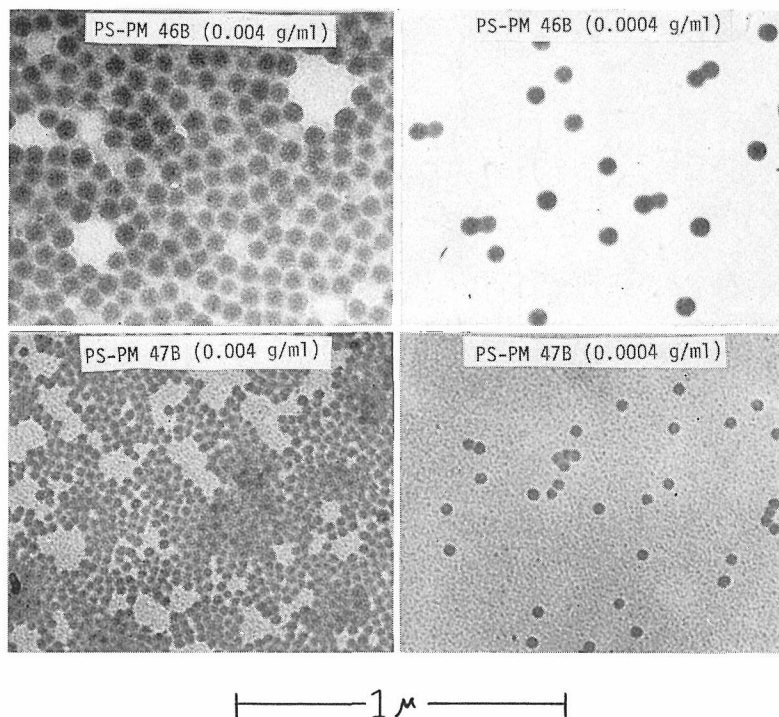


Fig. 1. Electron micrographs of the micelles from acetonitrile solutions of PS-PM diblock copolymers 46B ($M_w=3.4 \times 10^5$, and $x_{PS}=0.45$) and 47B ($M_w=1.09 \times 10^5$, and $x_{PS}=0.42$) with polymer concentration as indicated in the figures.

by the B chains were assumed to enter the core freely. It would be more realistic to assume that a micelle formed by a large number of molecules generally consists of three phases, *i.e.*, a pure B phase forming the core, an A-B intermixing phase which includes the A-B junctions, and a pure A phase forming the fringe which surrounds the shell and the core. This model is analogous to Meier's model⁴⁾ proposed as one of the three basic structures of block copolymer solids.⁵⁾ In this paper we calculate the P function of such a model on the basis of the random-flight statistics,⁶⁾ and discuss the method of analysis of experimental data based on the model. In order to avoid the complexity arising from the optical artefact, light scattering measurements have been often made with solvents isorefractive for one of the copolymer components.⁷⁻¹¹⁾ As to block copolymer micelles, such measurements have been made by Utiyama *et al.*¹²⁾ on the PS-PM/toluene (TOL)-furfryl alcohol (FAL) mixed solvent system in which the fringe component is "invisible", and by us^{3,13)} on the PS-PM/p-xylene and PS-PM and PM-PS-PM/TOL-p-cymene (pCY) mixed solvent systems in which the core component is "invisible". Our interest here is the latter type of systems. In the following, it is assumed that the core component is "invisible".

THE THREE-PHASE MODEL

Let f AB diblock copolymer chains, each consisting of N_A A segments and N_B B segments, form in a selectively bad solvent for the B component a spherical micelle as

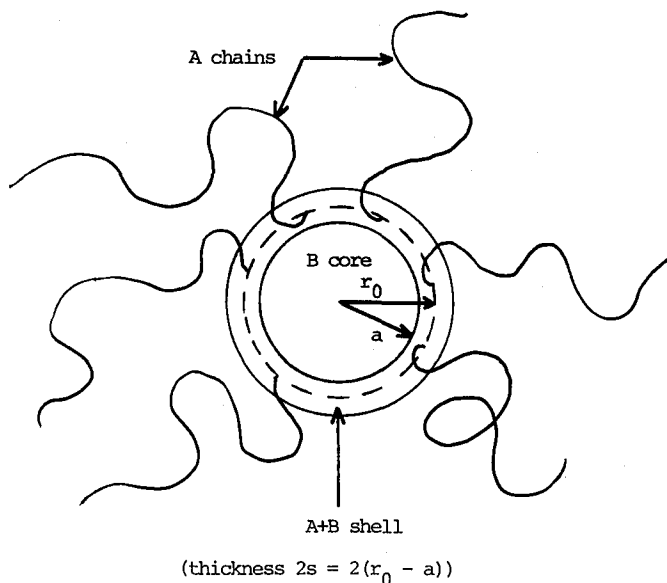


Fig. 2. Schematic representation of the "three-phase star-shape model."

illustrated in Fig. 2: The radius of the pure B core is a , and the thickness of the A-B intermixing phase is $2s$. For numerical simplicity, the A-B junctions are assumed to be in the middle of the intermixing phase, *i.e.*, on the surface of the sphere of radius $r_0 = a + s$, in a random manner. The A chains are assumed to obey the statistics of the random-flight chain with one end fixed at a radial distance $r = r_0$ and with an impermeable non-interacting boundary at $r = a$. No assumption is made here on the density distribution of B segments, since we have assumed that the B component is "invisible". This model will be designated as the "three-phase star-shape model". The previous "star-shape model" is the special case where $a = 0$. Below, we will often use the reduced quantities R_0 , A , S ($= R_0 - A$), and R instead of r_0 , a , s , and r , respectively. They are defined by

$$R_0 = \beta^{1/2} r_0, \quad A = \beta^{1/2} a, \quad S = \beta^{1/2} s, \quad \text{and} \quad R = \beta^{1/2} r \quad (1)$$

$$\beta = 3/(2N_A b_A^2) \quad (2)$$

where b_A is the effective length of A segments.

In this section, let us derive the radial density distribution ρ of A segments. The distribution $f_n(r_n)$ of the end-to-end vector \mathbf{r}_n of a random-flight chain with $n+1$ segments of length b serially numbered from 0 to n obeys the diffusion equation,

$$\partial f_n(\mathbf{r}_n) / \partial n = (b^2/6) \Delta^2 f_n(\mathbf{r}_n) \quad (3)$$

If f_n is spherically symmetrical, Eq. (3) becomes one-dimensional by the replacement, $p_n = r_n f_n$ ($r_n = |\mathbf{r}_n|$):

$$\partial p_n(r_n) / \partial n = (b^2/6) [\partial^2 p_n(r_n) / \partial r_n^2] \quad (4)$$

For the present purpose, Eq. (4) should be solved under the condition that the first (0-th) segment is at $r = r_0$ and all the segments exist in the region of $r > a$. The problem now is analogous to the one for the chain terminally bound near a planar surface.⁶⁾ Following

the similar procedure, we obtain the probability density $p_n(r_i/r_0|a)$ of finding the i th segment at r_i with the 0-th segment fixed at r_0 and all the segments found at $r > a$:

$$\begin{aligned} p_n(r_i/r|a) = & \{(r_0 - a)/r_0 + (a/r_0) \operatorname{erf}[\beta_{0n}^{1/2}(r_0 - a)]\}^{-1} \\ & \times (4\pi r_0 r_i)^{-1} (\beta_{0i}/\pi)^{1/2} \{\exp[-\beta_{0i}(r_0 - r_i)^2] - \exp[-\beta_{0i}(r_0 + r_i - 2a)^2]\} \\ & \times \{(r_i - a)/r_i + (a/r_i) \operatorname{erf}[\beta_{in}^{1/2}(r_i - a)]\} \end{aligned} \quad (5)$$

$$\beta_{lm} = 3/[2(m-l)b^2], \quad (l < m) = (0 < i < n) \quad (6)$$

$$\operatorname{erf} x = \int_0^x (2/\pi^{1/2}) \exp(-t^2) dt \quad (7)$$

where $\int_0^\infty p_n(r_i/r_0|a) (4\pi r_i^2) dr_i = 1$.

The overall radial density distribution $\rho_n(r/r_0|a)$ normalized to unity is given by

$$\rho_n(r/r_0|a) = (n+1)^{-1} \sum_{i=0}^n p_n(r_i/r_0|a), \quad r_i = r \quad (8)$$

Putting Eq. (5) in (8), converting the summation to an integral, and carrying out the integration,¹⁴ we have the following result:

$$\begin{aligned} \rho_{NA}(r/r_0|a) \times (4\pi r^2) &= (2\beta^{1/2}/\pi^{1/2}) [R_0 - A + A \operatorname{erf}(R_0 - A)]^{-1} \\ &\times \{R [\exp(-h_1^2) - \exp(-h_2^2) - \pi^{1/2} h_1 (1 - \operatorname{erf} h_1) + \pi^{1/2} h_2 (1 - \operatorname{erf} h_2)] \\ &+ A [-\exp(-h_3^2) + \exp(-h_4^2) + \pi^{1/2} h_3 (1 - \operatorname{erf} h_3) - \pi^{1/2} h_4 (1 - \operatorname{erf} h_4)]\} \end{aligned} \quad (9)$$

$$\begin{aligned} h_1 &= |R - R_0|, \quad h_2 = R + R_0 - 2A \\ h_3 &= |R - R_0| + R - A, \quad h_4 = 2R + R_0 - 3A \end{aligned}$$

where we have set $n = N_A$, and $b = b_A$ (*i.e.*, $\beta_{0n} = \beta = 3/(2 N_A b_A^2)$). In the particular case where $r_0 \rightarrow a$ (or $R_0 \rightarrow A$), Eq. (9) converges to¹⁵

$$\begin{aligned} \rho_{NA}(r/r_0 = a|a) \times (4\pi r^2) &= 4\beta^{1/2} (1 + 2A/\pi^{1/2})^{-1} \{R[1 - \operatorname{erf}(R - A)] - A[1 - \operatorname{erf}(2R - 2A)]\} \end{aligned} \quad (10)$$

CALCULATION OF THE PARTICLE SCATTERING FUNCTION

The apparent particle scattering function P_{app} for an A-B binary copolymer system is generally given by¹⁶

$$P_{app} = \mu_A^2 P_A + \mu_B^2 P_B + 2\mu_A \mu_B P_{AB} \quad (11)$$

$$\mu_A = 1 - \mu_B = x\nu_A / (x\nu_A + y\nu_B) \quad (12)$$

where P_K and P_{AB} describe the interference effects between K-K and A-B segments, respectively; x ($=1-y$) is the weight fraction of A segments, and ν_A is the refractive index increment of the K homopolymer (K=A or B). In our case, $\nu_B = 0$, so that $P_{app} = P_A$. P_A is conveniently split into the two terms $P_{A,1}$ and $P_{A,2}$, representing the inter- and intrachain contributions, respectively:

Table I. Values of $P_{A,1}^{1/2}$ for the "Three-Phase Model"^a

$S/R_0 \backslash X_{A,1}$	0.5	1.0	1.5	2.0	3.0	4.0	5.0	7.0	9.0	11.0	13.0
$R_0=0.0$											
	0.921	0.850	0.787	0.730	0.632	0.552	0.487	0.387	0.316	0.266	0.227
$R_0=0.1$											
1.0	0.921	0.850	0.787	0.730	0.632	0.551	0.485	0.385	0.314	0.262	0.223
0.8	0.921	0.850	0.786	0.729	0.630	0.549	0.482	0.380	0.307	0.255	0.216
0.6	0.921	0.850	0.786	0.728	0.628	0.546	0.478	0.374	0.301	0.247	0.207
0.4	0.921	0.849	0.785	0.727	0.626	0.543	0.473	0.369	0.294	0.239	0.198
0.2	0.921	0.849	0.784	0.726	0.624	0.540	0.471	0.363	0.287	0.231	0.190
0.0	0.921	0.849	0.784	0.725	0.622	0.538	0.467	0.358	0.280	0.223	0.181
$R_0=0.2$											
1.0	0.921	0.850	0.786	0.729	0.630	0.548	0.481	0.379	0.306	0.253	0.213
0.8	0.921	0.850	0.785	0.727	0.627	0.544	0.475	0.370	0.295	0.240	0.200
0.6	0.921	0.849	0.784	0.725	0.623	0.539	0.469	0.361	0.284	0.227	0.185
0.4	0.921	0.849	0.783	0.724	0.620	0.534	0.462	0.351	0.272	0.214	0.171
0.2	0.920	0.848	0.782	0.722	0.617	0.530	0.456	0.342	0.260	0.200	0.156
0.0	0.920	0.848	0.781	0.721	0.614	0.525	0.450	0.333	0.248	0.186	0.140
$R_0=0.3$											
1.0	0.921	0.850	0.785	0.727	0.627	0.544	0.475	0.370	0.294	0.239	0.198
0.8	0.921	0.849	0.784	0.725	0.623	0.538	0.468	0.359	0.281	0.224	0.181
0.6	0.921	0.848	0.783	0.723	0.619	0.532	0.460	0.347	0.266	0.207	0.163
0.4	0.920	0.848	0.782	0.721	0.615	0.526	0.452	0.335	0.251	0.190	0.144
0.2	0.920	0.847	0.780	0.719	0.611	0.520	0.444	0.323	0.236	0.172	0.125
0.0	0.920	0.847	0.779	0.717	0.608	0.515	0.436	0.311	0.221	0.155	0.106
$R_0=0.4$											
1.0	0.921	0.849	0.784	0.725	0.623	0.538	0.468	0.359	0.280	0.223	0.180
0.8	0.921	0.848	0.783	0.723	0.619	0.532	0.459	0.346	0.265	0.206	0.160
0.6	0.921	0.848	0.781	0.721	0.615	0.526	0.451	0.333	0.249	0.186	0.140
0.4	0.920	0.847	0.780	0.719	0.610	0.519	0.442	0.320	0.232	0.167	0.119
0.2	0.920	0.846	0.779	0.716	0.606	0.512	0.433	0.307	0.215	0.147	0.098
0.0	0.920	0.846	0.778	0.714	0.602	0.506	0.424	0.293	0.198	0.128	0.076
$R_0=0.5$											
1.0	0.921	0.848	0.783	0.723	0.619	0.532	0.459	0.346	0.265	0.205	0.160
0.8	0.920	0.848	0.781	0.721	0.615	0.526	0.451	0.334	0.249	0.187	0.140
0.6	0.920	0.847	0.780	0.719	0.611	0.519	0.442	0.320	0.232	0.167	0.118
0.4	0.920	0.846	0.779	0.716	0.606	0.512	0.432	0.306	0.214	0.146	0.096
0.2	0.920	0.846	0.777	0.714	0.602	0.505	0.423	0.292	0.196	0.126	0.074
0.0	0.920	0.845	0.776	0.712	0.597	0.499	0.414	0.278	0.178	0.105	0.051
$R_0=0.7$											
1.0	0.920	0.847	0.780	0.719	0.611	0.520	0.442	0.321	0.233	0.168	0.120
0.8	0.920	0.847	0.779	0.717	0.607	0.514	0.435	0.310	0.219	0.152	0.102
0.6	0.920	0.846	0.778	0.715	0.603	0.508	0.426	0.297	0.202	0.132	0.080
0.4	0.920	0.845	0.777	0.713	0.599	0.501	0.417	0.283	0.184	0.111	0.057
0.2	0.920	0.845	0.775	0.711	0.595	0.494	0.408	0.269	0.166	0.090	0.035
0.0	0.919	0.844	0.774	0.709	0.591	0.488	0.399	0.255	0.148	0.069	0.012
$R_0=1.0$											
1.0	0.920	0.846	0.777	0.713	0.600	0.503	0.420	0.288	0.191	0.120	0.068
0.8	0.920	0.845	0.776	0.712	0.598	0.500	0.415	0.280	0.181	0.108	0.055
0.6	0.920	0.845	0.775	0.711	0.595	0.495	0.408	0.269	0.166	0.090	0.035
0.4	0.919	0.844	0.774	0.709	0.591	0.488	0.400	0.256	0.150	0.071	0.013
0.2	0.919	0.844	0.773	0.707	0.587	0.483	0.392	0.244	0.134	0.052	-0.007
0.0	0.919	0.843	0.772	0.705	0.584	0.478	0.385	0.233	0.118	0.034	-0.027

^a $X_{A,1} = \omega^2 \langle S^2 \rangle_{A,1}$. For the values of $\langle S^2 \rangle_{A,1}$, see Table II. Value of $P_{A,1}^{1/2}$ reserves the sign of the rhs of Eq. (17), so that it can be negative in certain cases.

$$P_A = (1 - f^{-1})P_{A,1} + f^{-1}P_{A,2} \quad (13)$$

where f is the association number. The intrachain contribution $P_{A,2}$ may be sufficiently approximated¹⁷⁾ by the Debye function¹⁸⁾ for the linear free chain, *i.e.*,

$$P_{A,2} \sim (2/Y_A)^2 [\exp(-Y_A) - 1 + Y_A] \quad (14)$$

$$Y_A = \omega^2 / (4\beta) \quad (15)$$

$$\omega = (4\pi/\lambda) \sin(\theta/2) \quad (16)$$

where λ and θ have the usual significance. The interchain contribution $P_{A,1}$ is related to the density distribution ρ given by Eq. (9) as

$$P_{A,1}^{1/2} = \int_a^\infty 4\pi r^2 \rho_{NA}(r/r_0|a) \sin(\omega r) / (\omega r) dr \quad (17)$$

The integration cannot be analytically performed except for the case of $a=0$ (see footnote 19). Equation (17) was calculated with a FACOM 230-48 digital computer. A part of the results is listed in Table I.²¹⁾

The light scattering apparent mean-square radius $\langle S^2 \rangle_{app}$ derived from the ω^2 -term of the series expansion of P_{app} is likewise given by

$$\langle S^2 \rangle_{app} = \mu_A^2 \langle S^2 \rangle_A + \mu_B^2 \langle S^2 \rangle_B + 2\mu_A \mu_B \langle S^2 \rangle_{AB} \quad (18)$$

where $\langle S^2 \rangle_A$, $\langle S^2 \rangle_B$ and $\langle S^2 \rangle_{AB}$ concern P_A , P_B , and P_{AB} , respectively. In our case, $\langle S^2 \rangle_{app} = \langle S^2 \rangle_A$, and $\langle S^2 \rangle_A$ may be given by

$$\langle S^2 \rangle_A = (1 - f^{-1}) \langle S^2 \rangle_{A,1} + f^{-1} \langle S^2 \rangle_{A,2}, \quad (19)$$

$$\langle S^2 \rangle_{A,1} = \int_a^\infty 4\pi r^2 \rho_{NA}(r/r_0|a) dr \quad (20)$$

$$\langle S^2 \rangle_{A,2} \sim 1/(4\beta) \quad (21)$$

Equation (20) was calculated numerically.²²⁾ Table II lists the results.

Table II. Values of $\beta \langle S^2 \rangle_{A,1}$ for the "Three-Phase Model"^a

R_0/S	R_0	1.0	0.8	0.6	0.4	0.2	0.0
0.0		0.750					
0.1		0.760	0.783	0.808	0.834	0.862	0.892
0.2		0.789	0.831	0.877	0.930	0.988	1.054
0.3		0.840	0.894	0.959	1.037	1.129	1.236
0.4		0.909	0.974	1.055	1.157	1.284	1.438
0.5		0.999	1.069	1.164	1.290	1.453	1.661
0.6		1.110	1.181	1.288	1.436	1.637	1.903
0.7		1.239	1.312	1.427	1.600	1.836	2.166
0.8		1.389	1.461	1.582	1.773	2.050	2.448
0.9		1.560	1.627	1.754	1.963	2.280	2.750
1.0		1.751	1.814	1.943	2.168	2.526	3.073

^a $\beta = 3/(2N_A b_A^2)$.

ANALYSIS OF LIGHT SCATTERING DATA

In this section we describe what information is obtainable by analyzing, on the basis of the "three-phase model", light scattering data obtained for the core-component-invisible micelle system.

First, let us see the behavior of the model. In Fig. 3, $P_{A,1}^{-1}$ is plotted against $X_{A,1} = \langle S^2 \rangle_{A,1} \omega^2$ for several values of R_0 .²³⁾ The thickness of the intermixing phase was

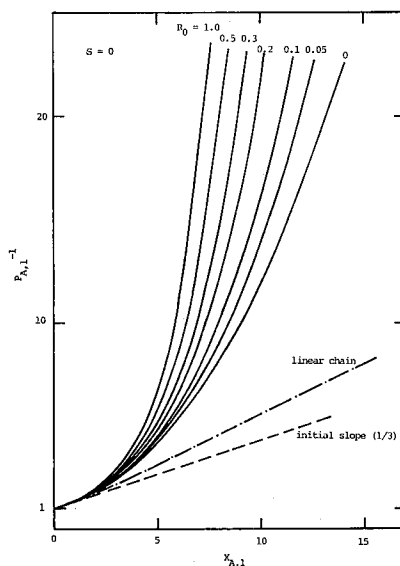


Fig. 3. Plots of $P_{A,1}^{-1}$ vs $X_{A,1}$ for the "three-phase star-shape model" with $S=0$, and R_0 as indicated in the figure: $X_{A,1} = \omega^2 \langle S^2 \rangle_{A,1}$.

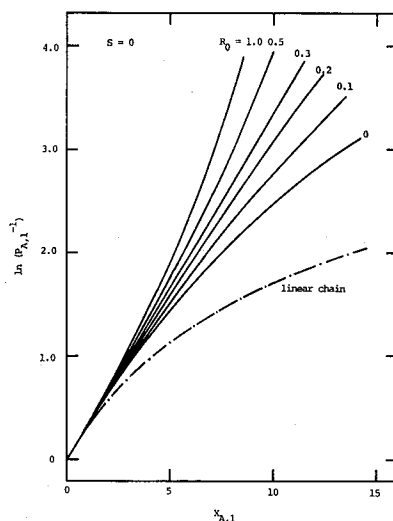


Fig. 4. Plots of $\ln P_{A,1}^{-1}$ vs $X_{A,1}$ for the "three phase star-shape model" with $S=0$, and R_0 as indicated in the figure: $X_{A,1} = \omega^2 \langle S^2 \rangle_{A,1}$.

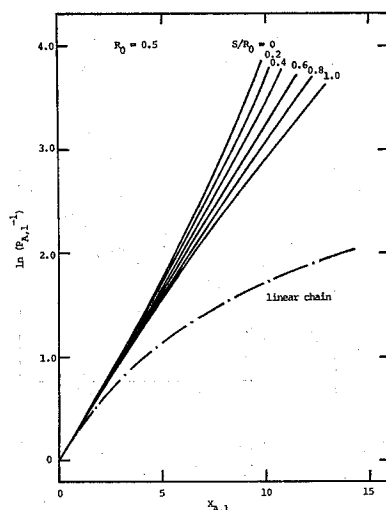


Fig. 5. Plots of $\ln P_{A,1}^{-1}$ vs $X_{A,1}$ for the "three-phase star-shape model" with $R_0 = 0.5$, and S/R_0 as indicated in the figure: $X_{A,1} = \omega^2 \langle S^2 \rangle_{A,1}$.

set zero, *i.e.*, $S = R_0 - A = 0$. The figure shows that $P_{A,1}^{-1}$ increases with increasing $X_{A,1}$ much more rapidly than that for a linear chain, showing large curvature at small $X_{A,1}$, *i.e.*, at low angles. The trend becomes more and more significant as R_0 increases. This is the characteristic common to spherical particles.³⁾ In a practical sense, the usual $Kc/R(\theta)$ vs $\sin^2(\theta/2)$ plot is no more effective to evaluate $\langle S^2 \rangle_{app}$ of a spherical micelle. In Fig. 4, the same data are presented in the $\ln P_{A,1}^{-1}$ vs $X_{A,1}$ plot. The curves have wider ranges of linearity at low angles. This plot appears to be the most favorable. In Fig. 5, $\ln P_{A,1}^{-1}$ is plotted against $X_{A,1}$ for several values of S/R_0 with R_0 fixed at $R_0 = 0.5$. We see that $P_{A,1}^{-1}$ becomes a somewhat slowly increasing function as S/R_0 increases.

Now, suppose that we have an experimentally determined P curve to be compared with the theoretical $P_{A,1}$ curve. The functional form of $P_{A,1}$ depends on the reduced quantities R_0 and S/R_0 alone (*cf.* Eqs. (9) and (17)). In principle, it is possible to determine the two by comparison. In practice, however, it appears almost impossible, since the theoretical curve for a given pair of R_0 and S/R_0 is reproduced by a number of other pairs almost perfectly at least in the region of $X_{A,1}$ of practical interest. For example, the curve for $R_0 = 0.3$ and $S/R_0 = 0$ closely fits the curve for $R_0 = S/R_0 = 0.5$ (*cf.* Fig. 4 and 5).

The fact is indeed noteworthy, however, that the pairs of R_0 and S/R_0 which give a common $P_{A,1}$ also give a common $\langle S^2 \rangle_{A,1}$, unless S/R_0 is not too large. If we set $\beta \langle S^2 \rangle_{A,1} = 1.5$, for example, all the curves for different pairs coincide with each other within $\pm 0.5\%$ up to $X_{A,1} = 15$, if $S/R_0 < 2/3$. As S/R_0 comes closer to unity, the deviation steeply becomes larger (about 20% at $X_{A,1} = 10$ for $S/R_0 = 1$). Under the assumption that S/R_0 is not so large (which does not sound unreasonable in view of the two-phase structures in bulk), the above fact points to a possibility to derive a new piece of information with less ambiguity. The procedure may be as follows: The observed P function is compared with the theoretical curves for, for example, $S/R_0 = 0$ (*i.e.*, Fig. 3 or 4), and the best fit value of R_0 is determined. The R_0 determines $\beta \langle S^2 \rangle_{A,1}$ (*cf.* Fig. 6). Thus, β can be known, since $\langle S^2 \rangle_{A,1}$ is, of course, known from the measured value of $\langle S^2 \rangle_A$ (*cf.* Eqs.

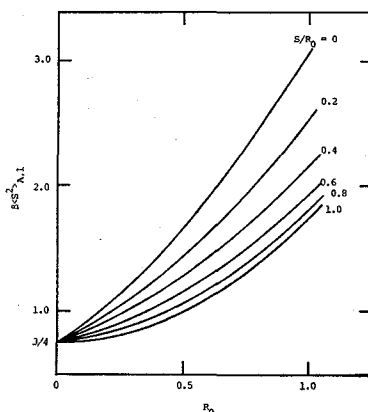


Fig. 6. Plots of $\beta \langle S^2 \rangle_{A,1}$ vs R_0 for the "three-phase star-shape model" with S/R_0 as indicated in the figure: $\beta = 3/(2N_A b_A^2)$.

(19–21)).

Here, some words may be necessary for the parameter β . In the absence of the excluded volume effects, β^{-1} ($= 2 N_A b_A^2/3$) is equal to $4 \langle S^2 \rangle_{A, \text{free}}$, where $\langle S^2 \rangle_{A, \text{free}}$ is the mean-square radius of the equivalent free A chain. In the presence of a positive excluded volume effect between A segments (which is usually the case with the micelle system), the equality no more holds. The A chains belonging to a micelle should be extended in the radial direction so as to avoid the mutual interference. Of course, our random flight-statistics do not strictly describe such chains, but should still be a valid approximation. All what we are saying is that the segment length b_A includes the excluded volume effects acting within the micelle (a uniform-expansion approximation), and is generally different from the length $b_{A, \text{free}}$ of the free chain. This defines the expansion factor α_M as

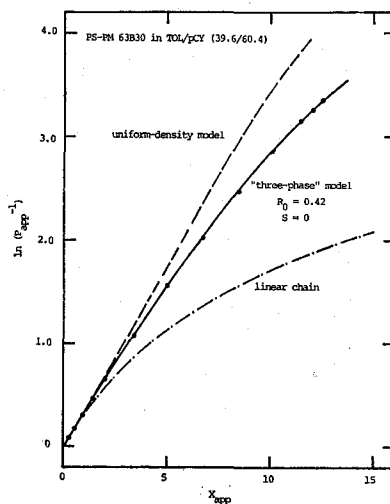


Fig. 7. Plots of $\ln P_{\text{app}}^{-1}$ vs X_{app} for PS-PM diblock copolymer 63B30 in a toluene/p-cymene mixture at 30°C (circles), for the "three-phase star-shape model" with $R_0 = 0.42$, and $S = 0$ (solid curve), and for the uniform-density model with $a = 0$ (broken curve): $X_{\text{app}} = \omega^2 \langle S^2 \rangle_{\text{app}}$.

$$\alpha_M = b_A / b_{A, \text{free}} \quad (22)$$

or equivalently

$$\alpha_M^2 = (4\beta \langle S^2 \rangle_{A, \text{free}})^{-1} \quad (22')$$

One should remind that α_M describes the expansion in the radial direction, and those in the other directions are, of course, undetectable by this method.

We show an example of such analysis. In Fig. 7, an experimental P_{app} curve¹³⁾ is compared with the theoretical curve for $S=0$ and $R_0=0.42$. The circles are measured points and the solid curve is the theory. The measurements were made on PS-PM diblock copolymer 63B30 ($M_w=1.5 \times 10^6$ and $x_{PS}=0.24$) with a TOL/pCY mixture (39.6/60.4 by weight) at 30°C. In this condition, only the PM chain is insoluble and, in addition, almost "invisible". Hence, the scattering comes predominantly from the PS chains which are forming the fringe. It was found that the apparent association number $f_{\text{app}}=79$, and $\langle S^2 \rangle_{\text{app}}^{1/2}=840 \text{ \AA}$. The f_{app} should be close to the true f , since the compositional heterogeneity in a copolymer sample should, if any, be smoothed out to a large extent in a multimolecular micelle. The PM has a small but finite visibility ($\nu_{PM}/\nu_{PS}=0.07$). The theoretical curve in Fig. 7 includes this effect in a suitable manner.²⁴⁾ As the figure shows, the agreement between the theory and the experiment is excellent. For the sake of comparison, we have shown the theoretical curve for the uniform-density model.¹²⁾ This model consists of a uniform-density B core of radius a surrounded by a uniform-density A shell of thickness $d-a$. The ratio of a to d determines the shape of the P function of this model. The broken curve in the figure shows the case of $a=0$. The agreement with the experiment is poor. If we assume a nonzero a , it becomes worse. The uniform-density model is unable to explain the experiment, whatever parameter we may choose.

Now, with the value of $R_0=0.42$ obtained above, we have $\beta \langle S^2 \rangle_{A,1}=1.47$ from Fig. 6. From the known value of $\langle S^2 \rangle_{\text{app}}$ and the independently determined value of $\langle S^2 \rangle_{A, \text{free}}^{1/2}=236 \text{ \AA}$, we have $\beta^{-1/2}=764 \text{ \AA}$, and the α_M given by Eq. (22) is estimated to be 1.62. This shows that the PS chains are significantly extended in the radial direction.

As pointed out above, it is not possible to estimate the "true" values of r_0 and s from this analysis alone. Together with the results for the fringe-component-invisible systems,¹²⁾ one would gain an answer to this question. Nevertheless, certain valuable information can be derived from the above analysis: The assumption of $S=0$ leads to the estimation that $r_0=\beta^{-1/2}R_0=321 \text{ \AA}$ from which the average density of the PM core is estimated to be 1.08 g/ml. This value is very close to the bulk density, and appears too high for the micelle density in solution. The PM core should be necessarily swollen to a certain extent. We expect that the true value of S/R_0 would be significantly larger than zero. If we assume that $0 > S/R_0 > 0.4$, for example, the possible range of R_0 becomes $0.42 > R_0 > 0.63$, giving the PM chains more room. Complete results on the PS-PM and PM-PS-PM/TOL-pCY systems will be given elsewhere.²⁵⁾

ACKNOWLEDGMENT

The electron micrographs were taken by Mr. M. Ohara of this Institute, who is gratefully acknowledged.

REFERENCES AND NOTES

- (1) See, *e.g.*, G. E. Molau, in "Block Polymers", S. L. Aggarwall. Ed., Plenum Press, New York, 1970.
- (2) To take the micrographs, a drop of the dilute solution was placed on a film, and the solvent was allowed to evaporate off (which occurred in a short time due to high volatility of the solvent). The adsorption behavior of iodine onto the dry micelle indicated that the micelle surface is covered with the PM chains: T. Tanaka, T. Kotaka, and H. Inagaki, *Polymer Preprints, Japan*, **19**, 561 (1970).
- (3) T. Tanaka, T. Kotaka, and H. Inagaki, *Polymer J.*, **3**, 327 (1972).
- (4) D. J. Meier, *J. Polym. Sci., Part C*, **26**, 81 (1969).
- (5) See, *e.g.*, T. Inoue, T. Soen, T. Hashimoto, and H. Kawai, *J. Polym. Sci., Part A-2*, **7**, 1283 (1969).
- (6) T. Tanaka, *Macromolecules*, **10**, 51 (1977).
- (7) M. Leng and H. Benoit, *J. Polym. Sci.*, **57**, 263 (1962).
- (8) J. Prud'homme and S. Bywater, *Macromolecules*, **4**, 543 (1971).
- (9) H. Utiyama, K. Takenaka, M. Mizumori, and M. Fukuda, *ibid.*, **7**, 28 (1974).
- (10) T. Tanaka, T. Kotaka, and H. Inagaki, *ibid.*, **7**, 311 (1974).
- (11) T. Tanaka, T. Kotaka, and H. Inagaki, *ibid.*, **9**, 561 (1976).
- (12) H. Utiyama, K. Takenaka, M. Mizumori, M. Fukuda, Y. Tsunashima, and M. Kurata, *ibid.*, **7**, 515 (1974).
- (13) T. Kotaka, T. Tanaka, M. Hattori, and H. Inagaki, *Polymer Preprints, Japan*, **25**, 1269 (1976).
- (14) The integration can be made through the Laplace folding operation.
- (15) D. J. Meier, private communication, 1975.
- (16) See, *e.g.*, H. Benoit and D. Froelich, in "Light Scattering from Polymer Solutions," M. B. Huglin, Ed., Academic Press, New York, 1972.
- (17) This approximation is justified to a certain extent by the fact that the mean-square radius of a chain terminally bound near a surface is close to that of the free chain (see ref. 6).
- (18) P. Debye, *J. Chem. Phys.*, **51**, 18 (1947).
- (19) When $a=0$, we have

$$P_{A,1}^{1/2} = \sin U_B [1 - \exp(-Y_A)] / (U_B Y_A), \quad U_B = r_0 \omega$$

This equation with Eqs. (13) and (14) recovers the P_A for the previous "star-shape model", which further reduces to the function for the regular star chains²⁰ if we set $r_0=0$. However, due to the approximation employed, the previous expression is different: $\exp(-U_B^2/3)$ in Eq. (17) of ref. 3 should be replaced by $[(\sin U_B)/U_B]^2$ to obtain the correct result given here.

- (20) H. Benoit, *J. Polym. Sci.*, **11**, 50 (1953).
- (21) A more complete list is available upon request.
- (22) Analytical results for particular cases are: for $r_0 \rightarrow a$,

$$\beta \langle S^2 \rangle_{A,1} = 3/4 + R_0^2 + (7/3)\pi^{-1/2} R_0 \times [1 + (9/14)\pi^{1/2} R_0] / (1 + 2\pi^{-1/2} R_0),$$

and for $a=0$,

$$\beta \langle S^2 \rangle_{A,1} = 3/4 + R_0^2.$$

- (23) It is noted that $P_{A,1} \sim P_A$ and $\langle S^2 \rangle_{A,1} \sim \langle S^2 \rangle_A$, if f is sufficiently large (cf. Eqs. (13) and (19)).
- (24) We have assumed a uniform density for the B core:

$$P_B^{1/2} = (3/U_B^3) (\sin U_B - U_B \cos U_B), \quad U_B = a\omega (=r_0\omega)$$

It will be obvious that P_{AB} , $\langle S^2 \rangle_B$ and $\langle S^2 \rangle_{AB}$ are given by

$$P_{AB} = P_{A,1}^{1/2} P_B^{1/2}$$

$$\langle S^2 \rangle_B = (3/5)a^2$$

$$\langle S^2 \rangle_{AB} = (1/2) (\langle S^2 \rangle_{A,1} + \langle S^2 \rangle_B)$$

- (25) T. Kotaka, T. Tanaka, M. Hattori, and H. Inagaki, to appear in *Macromolecules*.